PERGAMON

Journal of Geodynamics 29 (2000) 125-139

JOURNAL OF
GEODYNAMICS

Lithospheric seismic structure of the eastern region of the Arabian Peninsula

Abdullah M. Al-Amri*, Ali A. Gharib

Seismic Studies Center, King Saud University, Riyadh, 11451, Saudi Arabia Received 11 November 1998; received in revised form 15 January 1999; accepted 18 January 1999

Abstract

The lithospheric structure of the eastern region of the Arabian Peninsula has been derived using the spectral analysis of intermediate period P-wave amplitude ratios. Sixteen earthquakes recorded at the intermediate 3-component DHR station during the period from 1986 to 1995 were selected for analysis based on the following criteria: focal depths with a range between 15 and 300 km, body-wave magnitudes greater than 5.0, epicentral distances with a range from 13° to 82°.

By comparing the spectral peak positions of the observed and theoretical values, the thickness and velocity can be resolved within 3 km and 0.3 km s^{-1}, respectively of the observed values. Earthquakes from the Eurasian plate, Japan and China show high cross-correlation ratios (> 85%) and events from the Arabian plate, gulf of Aqabah, Red and Mediterranean Seas indicate cross-correlation ratios between 60-84%.

The derived crustal model is not unique due to the theoretical assumptions (horizontal layering, constant densities and velocities in each layer), quality of the data and complexities of the crustal structure. The model suggests that the crust consists of five distinct layers with a strong velocity gradient of about 0.05 km s^{-1} km^{-1} in the upper crust and 0.03 km s^{-1} km^{-1} in the lower crust. The average results for several observations give a crustal thickness of 51 km and, a mean P-wave velocity of 6.2 km s^{-1}. Depth to the crystalline basement is approximately 8 km which is in good agreement with values obtained by some oil wells in the eastern region. The Mohorovicic discontinuity indicates a velocity of 8.3 km s^{-1} of the upper mantle and 51 km depth.

* Corresponding

0264-3707/00/$ - see front matter Q 1999 Elsevier Science Ltd. All rights reserved. P11: 50264-3707(99)00006-X

1. Introduction

The Arabian platform makes up about two thirds of the Arabian Peninsula. It includes the interior homocline and the interior platform and basins. The width of the interior platform ranges from 100 km along the southern and western parts of the Rub'al Khali basin to 400 km south of Dhahran. The platform consists of Paleozoic and Mesozoic sedimentary rocks that unconformably overlie the Arabian shield and dip very gently to the E–NE towards the Arabian Gulf. Several major anticlines are superimposed, encompassing the major Arabian oil fields. Salt basins were found from early Cambrian, which affected the structure by salt diapir-type movements (Powers et al., 1966).

The importance of conducting this study is related primarily to the importance of the study area, which can be summarized in three points:

1. There is not a great deal known about the crustal structure beneath the eastern region of Saudi Arabia,

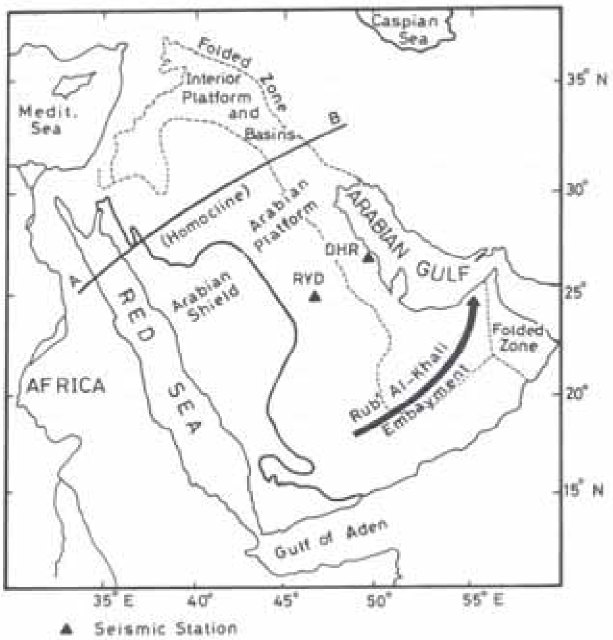

Fig. 1. Index map of the Arabian Peninsula showing major tectonic features of the Arabian shield and platform (Homocline, Interior platform and basins).

2. Dhahran is located in the easternmost part of the interior platform and surrounded by major oil fields (Fig. 1), which implies that deep crustal studies are of great importance from economic and academic viewpoints, and
3. Most if not all of the crustal structure studies conducted in the Arabian shield and platform have been based on the deep seismic refraction profile (Mooney et al., 1985). It begins about 85 km southwest of Riyadh (Fig. 1) in Paleozoic and Mesozoic cover rocks and leads southwesterly across major Precambrian tectonic provinces.

The purpose of this paper is to determine the lithospheric structure of the eastern Arabian platform from spectral analyses of intermediate period P-wave amplitude ratios.

Sixteen earthquakes (Table 1) which were recorded at DHR station between 1986 and 1995 and meet certain requirements and criteria have been utilized: body-wave magnitudes are greater than 5.0, focal depths from 15 to 300 km, epicentral distances range from 13° to 82°, and clear impulsive first P-wave onsets are recorded at the 3-components.

The spectral method has been widely used in studying the parameters of the crust and in examining the effect of surface layers on the amplitude variations. The theoretical background of this method was presented by Thomson (1950) and Haskell (1953) as a matrix formulation. The body wave spectral techniques make use of the Thomson–Haskell matrix method. The theoretical spectra, which were obtained from the horizontally layered earth models, are compared to the observed ones.

Phinney (1964) used Haskell's matrix method to calculate the spectral response of a layered crust to compare observed long period P-wave spectra from distant earthquakes. By taking the ratio of the vertical spectrum to the horizontal one he obtained a function that depended on the structure beneath the station. The usefulness of the spectral ratio method of deducing

Table 1
Source parameters of sixteen earthquakes that were used for the analysis

Location	Date (D. M. Yr)	Lat. (N)	Long. (E)	Dist. (Deg)	Depth (km)	m_b	Azimuih (Deg)	Depth to Moho	Corr. coeff.
Japan	10 02 89	02.311	126.76	77	44	6.2	94	49 ± 3	79%
Japan	12 05 90	49.04	141.85	72	300	6.5	44	51 ± 2	81%
Ethiopia	16 03 93	11.62	41.99	16.5	16	5.6	209	50 ± 3	76%
Egypt	12 10 92	29.62	31.00	17	30	5.8	285	55 ± 3	77%
Med. Sea	21 11 92	35.92	22.49	25.5	65	5.9	299	53 ± 2	83%
Philippine	17 05 92	7.24	126.64	75	33	6.2	89	49 ± 3	78%
Burma	18 05 87	25.27	94.20	39.5	50	5.7	81	48 ± 3	70%
Iran	11 07 86	29.96	51.58	3.9	10	5.7	19	49 ± 2	90%
Philippine	17 05 92	7.24	126.64	75	33	6.2	89	42 ± 3	77%
Japan	06 02 87	36.99	141.79	76	36	5.9	55.6	52 ± 3	70%
Red Sea	13 03 93	19.63	38.80	12	10	5.9	240	52 ± 3	70%
Romania	30 05 90	45.84	26.67	27	89	6.7	322	48 ± 3	72%
Sudan	20 05 90	05.12	32.15	27	15	6.7	222.3	52 ± 2	80%
Afgh	26 09 88	36.29	71.37	21	107	5.6	56	49 ± 3	75%
China	29 04 87	39.76	74.57	24.4	10	6.4	50.5	54 ± 2	80%
Iran	30 03 88	30.89	50.19	4.6	33	5.4	0.5	49 ± 3	71%

crustal structure lies in the fact that the ratio of the vertical to horizontal Fourier components of a teleseism is independent of the signal spectrum and depends only upon the crustal structure and the angle of incidence of the plane wave (Hasegewa, 1971).

The method was successfully utilized by many investigators. Bonjer et al. (1970) studied the crustal structure under the East African Rift system. Hasegewa (1971) studied the structure under the Yellowknife area in Canada. Turkelli (1984) made use of the digital P-wave data of Seismic Research Observatories (SRO) station to determine the crustal structure in central Anatolia using the matrix formulation. Ellis and Basham (1968) concluded that horizontal layers do not fulfill the requirements of the Thomson–Haskell matrix theory for testing short period P-waves because of the scattering and anomalies due to P–S conversion in the crust and upper mantle.

More recently, Al-Amri et al. (1996) and Al-Amri (1998, 1999) used the spectral analysis of long-period amplitude ratios to derive the crustal structure of the Arabian shield and the Arabian platform. Lithospheric velocity structure of the Arabian shield and platform has been determined using teleseismic receiver function deconvolution techniques (Sandvol et al., 1998), regional wave form modeling and surface wave group velocities (Rodgers et al., 1999). Regional waveform propagation is characterized in the Arabian Peninsula using stacking techniques (Mellors et al., 1999).

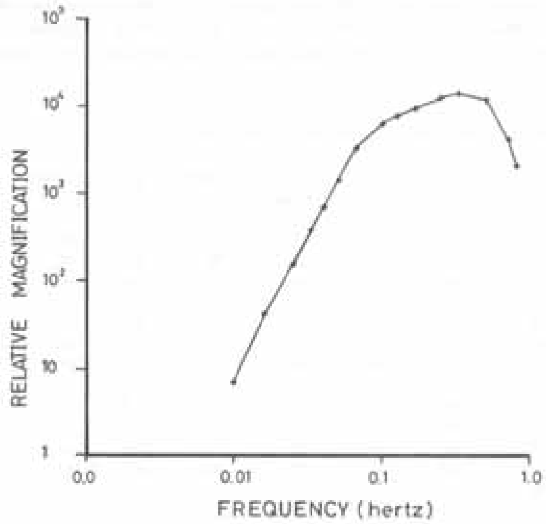

Fig. 2. Analog system response curves for the Dhahran (DHR) station. The intermediate period response curve extends from 0.01 to 0.8 Hz.

2. Earthquake data treatment

The Dhahran (DHR) station of King Fahd University of Petroleum and Minerals (Fig. 1) is a 6-channel station located at lat. 26.30° N. and long. 50.14° E. The station consists of three component short period and three component intermediate period seismometers oriented in the vertical, N–S and E–W directions. The intermediate period response curve for DHR station extends from a round 0.016 to 0.8 Hz (Fig. 2) and the sampling rate of 4.26 per second of real time gives a Nyquist frequency of 2.14 Hz, which is above the frequency range of interest for intermediate period spectral ratio studies. It means that the Nyquist frequency can not cause

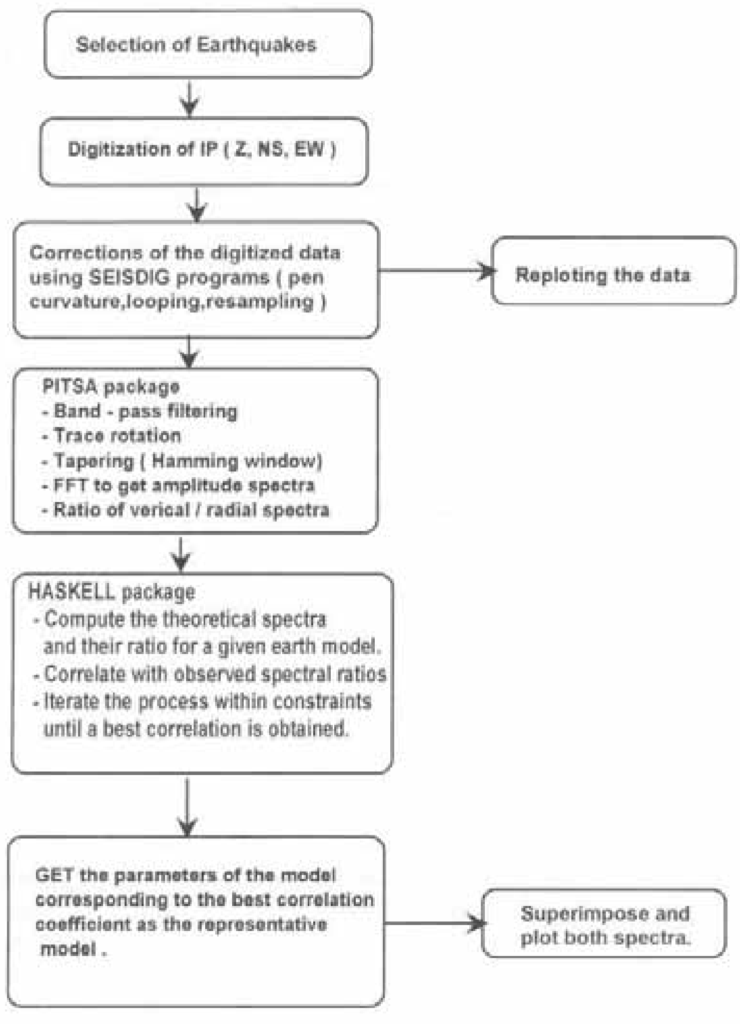

Fig. 3. Flowchart showing earthquake data treatment and analytical procedure.

aliasing. The upper frequency limit of 0.8 Hz is sufficient to include all frequencies which can be reasonably investigated using standard intermediate period recordings at DHR station.

The intermediate-period three component seismograms of DHR station are digitized by hand. The digitization includes several steps: seismogram preparation and manipulation, calibration of seismogram for time and amplitude scale, digitization of the traces and related time marks. The length of the digitization window is not less than two minutes with three time marks and it is the same for 3 components.

The analysis of the digitized seismograms was carried out using the PITSA program package (IASPEI, 1990). The three components seismogram for each earthquake were treated identically. The seismic traces were filtered with a band-pass filter whose corner frequencies matched the instrument response curve (Fig. 2). Hamming window was applied to minimize the later arrivals after the P-wave. Fig. 3 shows a flowchart of processing and treatment of earthquake data.

The spectral analyses were based on the matrix method of Thomson–Haskell in which theoretical spectra obtained from the horizontally layered earth models are compared with the observed spectra. For the method be of practical use, the theoretical curves must be neither too sensitive nor too insensitive to changes in the model parameters. Enough data must also be collected so that they can be assessed for repeatability and variability.

The spectral amplitude of vertical $\mathrm{Z}(\omega)$ and horizontal $\mathrm{H}(\omega)$ components are obtained using FFT algorithm of the package. The ratio of the spectra of Z and R is obtained using the trace utilities menu of the PITSA (IASPEI, 1992) and can be written as:

$$\mathrm{Z}(\omega) = A_0(\omega) \cdot C_z(\omega) \cdot I(\omega) \tag{1}$$

and

$$\mathrm{H}(\omega) = A_0(\omega) \cdot C_h(\omega) \cdot I(\omega), \tag{2}$$

where $C_z(\omega)$ and $C_h(\omega)$ are the vertical and horizontal crustal transfer functions computed by the matrix formulation, $A_0(\omega)$ is the body wave spectrum incident at the base of the crust, and $I(\omega)$ is the amplitude response of the recording system. Because the instrument responses of both vertical and horizontal seismograph systems are the same, we can eliminate them by dividing $\mathrm{Z}(\omega)$ by $\mathrm{H}(\omega)$ and obtaining the theoretical crustal transfer ratio, $\mathrm{T}(\omega)$, which is independent of $A_0(\omega)$ (Hasegewa, 1971).

$$\mathrm{T}(\omega) = \frac{\mathrm{Z}(\omega)}{\mathrm{H}(\omega)} = \frac{C_z}{C_z}. \tag{3}$$

It is generally assumed that the earth's crust is made of horizontal, homogeneous and isotropic layers with a system function that can be used to find the response of the crustal structure. In practice, for known horizontal and vertical component ground motion the left hand side of Eq. (3) can be computed and compared with the right hand side which represents the theoretical transfer function of a particular crustal model. In the actual case, dipping layers are present and may influence the crustal transfer functions. Some of the discrepancies between the observational and theoretical curves may be due to the complexities of the crustal structure and to the quality of the analog data used.

Since some epicentral distances are less than 30°, there are complexities and ambiguities in the appearance of the seismograms due to some phase interferences. Consequently, all seismograms were carefully checked and selected the clearest P-wave onset to avoid such complexities.

3. Results and discussion

The spectral technique used in this study requires assumptions to be made (horizontal layering, constant densities and velocities in each layer). The vertical velocity gradient is taken into the problem by making the model with many layers, beginning with constant velocities in each layer.

The generation of the theoretical spectra requires an earth model. This paper started out with the previously determined two models for the western part of the Arabian platform. The first model (Badri, 1991) is based on 2-D ray path interpretation of travel time and wave amplitude ratios of the 1978 USGS seismic refraction data. He showed that the crust consists of four distinct layers approximately 41 km-thick under the Arabian platform. The upper crust has a P-wave velocity of about 5.9 km s^{-1} and is about 3 km thick. The second layer has a P wave velocity of about 6.2 km s^{-1} and is about 7 km-thick. The third crustal layer has a Pwave velocity of about 6.4 km s^{-1} and is about 16 km thick. The lower crust has a P-wave velocity of 6.8 km s^{-i} and is 15 km thick.

The second model (Al-Amri, 1998) was derived using the spectral analysis of long-period Pwave amplitude ratios to investigate the crustal structure beneath the Arabian platform. His model suggests that the crust consists of five distinct layers with a total thickness of 42 km and a P-wave velocity of 8.2 km s^{-1} of the upper mantle.

By adding a thick layer of 8 ± 1 km, and a P-wave velocity of 4.8 ± 0.3km s^{-1} at the top of Badri's crustal model (1991), to check the reliability of the initial two models (Badri, 1991; AlAmri, 1998). The results show a better cross-correlation for the 5-layer model rather than the 4-layer model between the theoretical and observed spectra. The 5-layer model has been tested to develop theoretical models to compare with the observed crustal transfer function of the 16 earthquakes, assuming no lateral variations and dipping in the velocity structure. Several theoretical models are obtained for each earthquake. The selection of the most suitable model was based on the identification of the theoretical model which exhibits the highest cross correlation coefficient with the observed transfer function ratio.

The resolution of the spectral ratio method and the effect of different model parameters on the theoretical spectra were tested by first keeping the thickness of the first layers constant and varying the velocities. Then the velocities were kept constant but the thicknesses varied. Accordingly, our model assumes that the crust consists of five distinct layers approximately 51 km thick, with an average P-wave velocity of 6.3 km s^{-1}. This model was derived by allowing both layer velocities and thicknesses of each crustal layer to vary ±0.3 km s^{-1} and ±2 km, respectively until a theoretical model fitted the observed data. By comparing the spectral peak positions of the theoretical and observed values, the velocity and thickness can be resolved within 0.3 km s^{-1} and 3 km, respectively, of the observed values. Little changes had to be made in the parameters to obtain the best correlation coefficients. However, these variations were constrained by the lithological conditions.

The derived final model is calculated using 16 events Table 1 with epicentral distances that range between 13° and 82°. By increasing the P-velocity from 6.3 to 6.6 km s^{-1} and keeping the total crustal thickness constant at 51 km-depth (Fig. 4), the spectral amplitude ratios decrease and the frequencies shift from 0.55 to 0.61 Hz and by decreasing the P-velocity to 6.0 km s^{-1}, the spectral ratios increase and the frequencies shift from 0.55 to 0.5 Hz.

On the other hand, increasing the total depth from 51 to 52 km (Fig. 5) shifts the peak from 0.55 to 0.45 Hz and from 0.55 to 0.5 Hz in case of decreasing the depth from 51 to 50 km.

The results indicate that events from Iran (Fig. 6), Afghanistan, China and Japan were considered to obtain a crustal model with a correlation coefficient between observed and theoretical above 85%, whereas earthquakes from the Arabian plate, the Red Sea (Fig. 7) and the Mediterranean Sea, gulf of Aqabah, Egypt and Turkey show correlation coefficients between 60% and 84%. Smaller values of the correlation coefficients reflect discrepancies between the theoretical and observed transfer function. Existence of some peaks at the beginning of the observed spectra (Figs. 6 and 7) could be due to one of the following reasons: 1. tilting effect on the seismometers, 2. low signal to noise ratio at DHR station, 3.

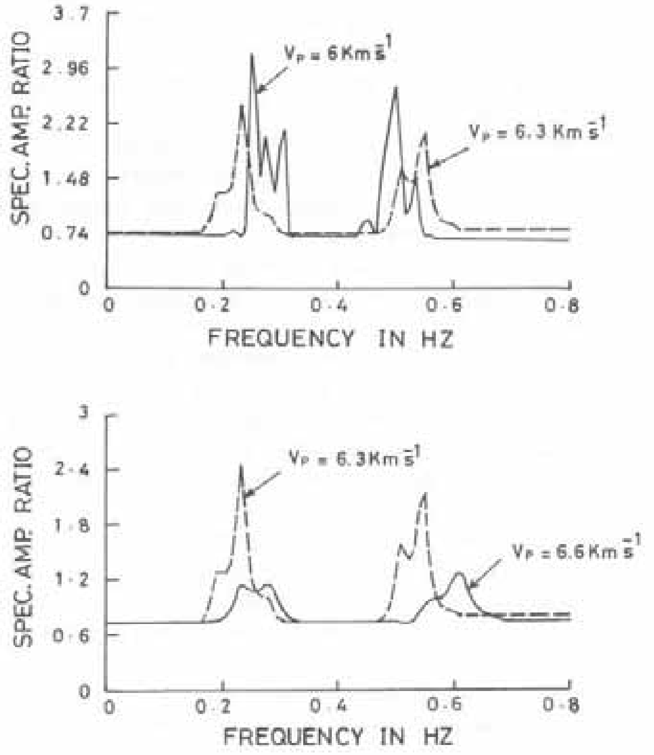

Fig. 4. Variations of the theoretical transfer function ratio with respect to the seismic velocities.

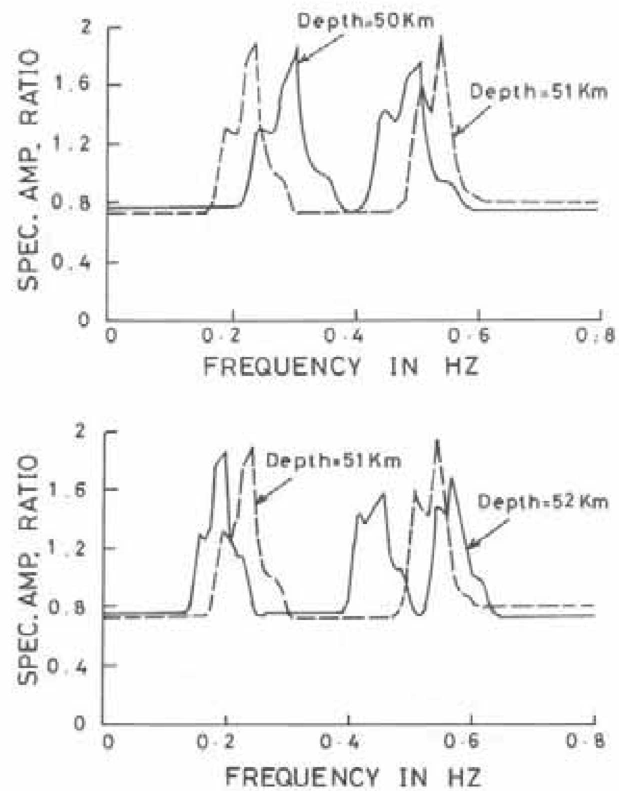

Fig. 5. Variations of the theoretical transfer function ratio with respect to the total crustal thickness.

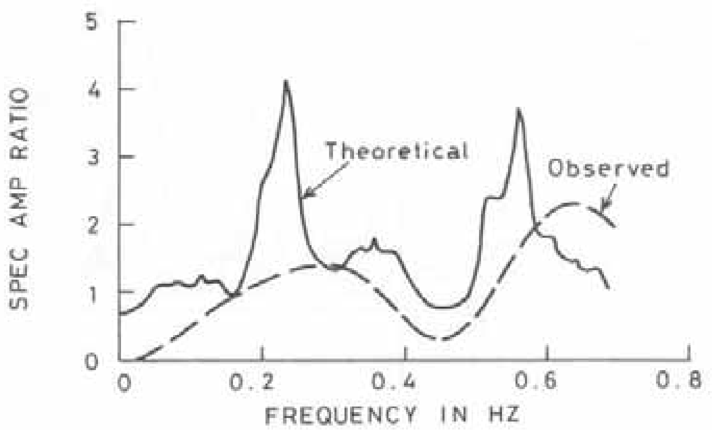

Fig. 6. Plots of theoretical and observed spectral ratio for earthquake of March 30, 1988 (Iran) and relevant information together with obtained crustal model.

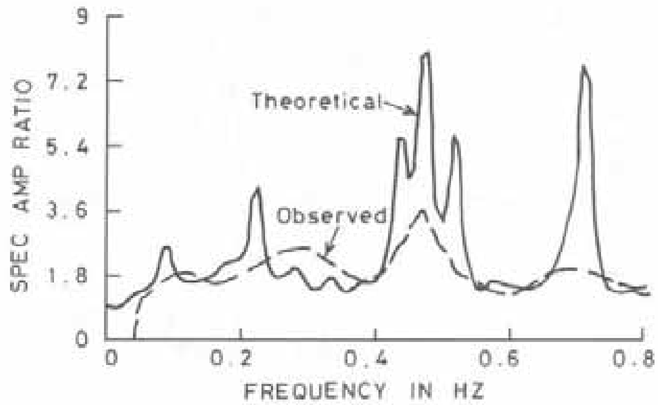

Fig. 7. Plots of theoretical and observed spectral ratio for earthquake of March 13, 1993 (S. Red Sea) and relevant information together with obtained crustal model.

contamination of diffracted P-waves when the epicenter has a large distance or due to the complications of the near earthquake pP phases.

The observed spectra at RYD and DHR intermediate periods for the earthquake of Oct. 12, 1992 (Egypt) is superimposed in Fig. 8. The highest spectral peak moves towards high frequencies (0.7 Hz) for RYD indicating a thinner crust and the highest peak at DHR moves towards lower frequencies (0.5 Hz) indicating thicker crust. Similarly, the observed spectral ratios in Fig. 9 for the earthquake of April 30, 1987 (China) show that the highest spectral peak moves towards high frequencies (0.75 Hz) for RYD indicating thinner crust and the highest peak at DHR moves towards lower frequencies (0.55 Hz) indicating thicker crust.

Since only one station was used, and in order to obtain a good number of observations,

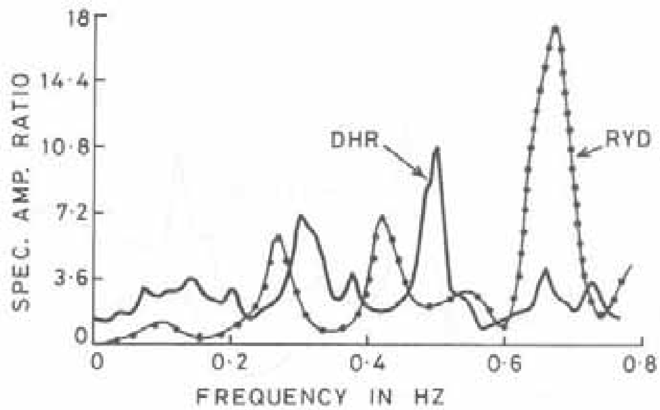

Fig. 8. Comparison between the observed spectra at RYD and DHR intermediate periods for earthquake of Oct. 12, 1992 (Egypt). The curve with closed circles denotes for RYD and the curve without circles for DHR. The highest spectral peak moves towards high frequencies (0.7 Hz) for RYD indicating thinner crust and the highest peak at DHR moves towards lower frequencies (0.5 Hz) indicating thicker crust.

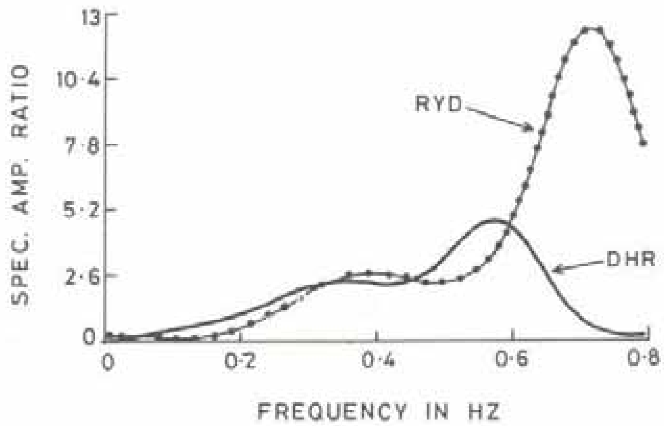

Fig. 9. Comparison between the observed spectra at RYD and DHR intermediate periods for earthquake of April 30, 1987 (China). The curve with closed circles denotes for RYD and the curve without circles for DHR. The highest spectral peak moves towards high frequencies (0.75 Hz) for RYD indicating thinner crust and the highest peak at DHR moves towards lower frequencies (0.55 Hz) indicating thicker crust.

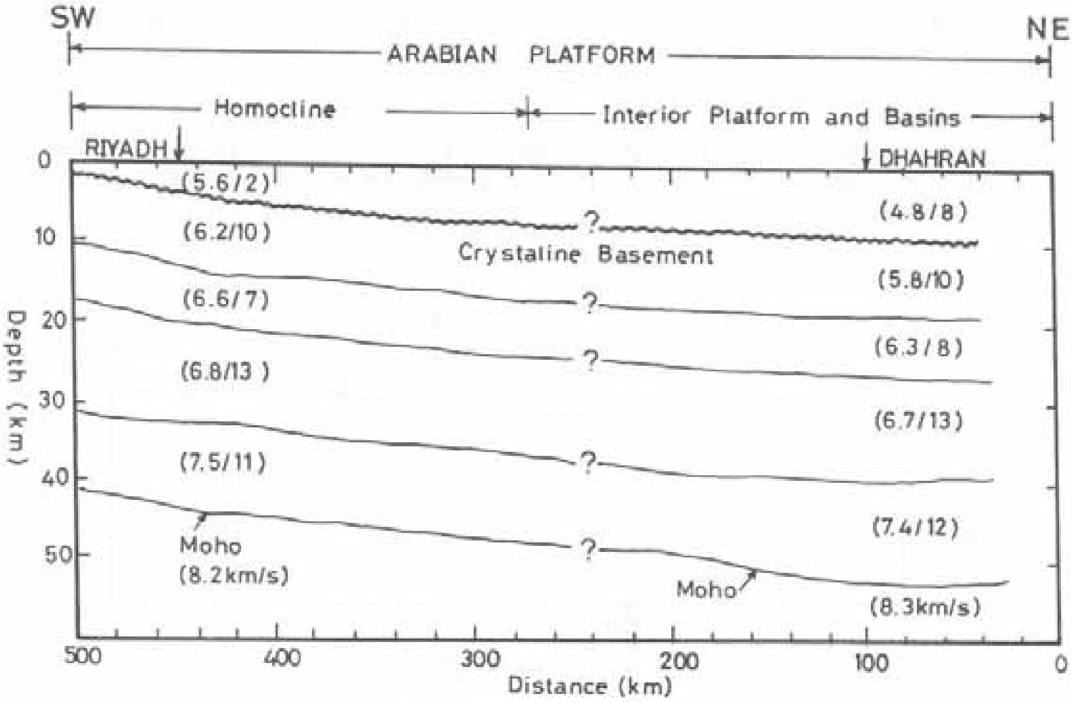

Fig. 10. Composite cross-section of the crust and upper mantle of the entire Arabian platform (homocline, interior platform and basins) beneath RYD and DHR stations. Depth to the basement and Moho increases towards northeast. Numbers in parentheses indicate values of velocity in km s^{-1} and thickness in km, respectively.

sixteen earthquakes were carefully examined. By comparing the peak positions of the observed and theoretical spectral curves, we can resolve the crustal thickness and average velocity within 3 km and 0.3 km s^{-1}, respectively, of the observed values. The sensitivity of the transfer functions to the changes of model parameters indicates that the peak at the lowest frequency is directly related to the total thickness of the crust. Thicker crust shifts the position of the peak to lower frequencies and the higher the velocity contrast the higher the amplitudes and vice versa. A peak response at 0.68 Hz (Figs. 8 and 9) is shifted towards higher frequencies. This may indicates a thinner crust under the western Arabian platform (beneath RYD).

In comparison with previous crustal models (Badri, 1991; Mokhtar et al., 1992; Al-Amri, 1998), this model shows clear velocity boundaries. The Mohorovicic discontinuity varies from a depth of 46 km and upper mantle velocity of 8.2 km s^{-1} in the southwest direction beneath Riyadh station (Fig. 10) to a depth of 51 km and upper mantle velocity of 8.3 km s^{-1} in the northeast direction beneath Dhahran station (both stations are located in the Arabian platform).

It is interesting to note that depth to the crystalline basement (Fig. 10) varies gently from 3 to 8 km under Riyadh and Dhahran. The 3 km-depth to the basement beneath Riyadh is in good agreement with the depth to the basement found from oil wells in the region (Peterson and Wilson, 1986). The platform is covered by Phanerozoic sediments which gradually thicken to nearly 10 km in the Mesopotamian foredeep and Arabian gulf (Seber et al., 1997). They indicate that the thickest crust occurs beneath the Zagros mountains in Iran where continental collision is taking place and the thinnest crust occurs beneath the southern Red Sea where new oceanic crust is forming (Fig. 11). The Mesopotamian foredeep is identifiable by the thickening of sedimentary rock toward the Zagros collision zone. By following the 1500 m elevation contour on the high-resolution topographic image, Seber et al. (1997) mapped the boundary of Turkish and Iranian plateau using digital elevation models (DEM). This contour represents the maximum elevation of the plateau that defines a continuous elevated surface over the entire region.

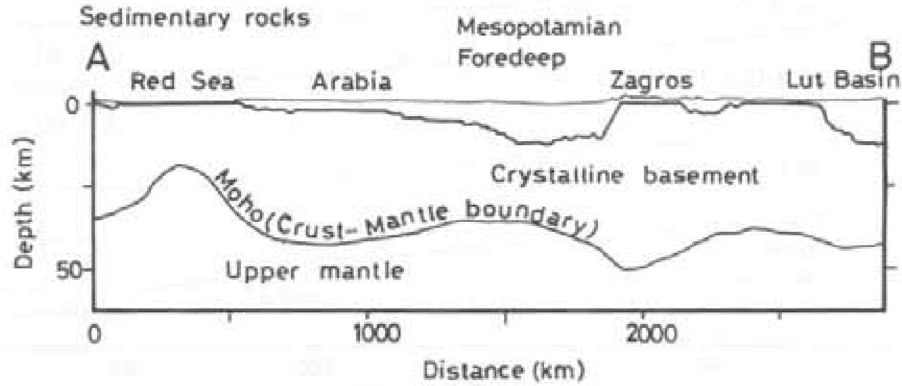

Fig. 11. Crustal structure profile showing how the crust–mantle boundary and the thickness of sedimentary cover change across the Red Sea, the Arabian plate and the Zagros suture (Seber et al., 1997) as shown in Fig. 1 (line A–B). Depth to the Moho or base of the crust is largerly based on seismic velocity information. The boundary between sedimentary cover and crystalline basement is set where seismic P-velocities reach 6 km s^{-1}.

Mooney et al. (1985) mapped the basement surface beneath the sediments of the western section of Arabian platform and indicated that the offsets due to faulting are of the order of 1000 m and maximum thickness of sediments obtained was about 1.75 km. Structural drills and reflection seismic data indicate that the sedimentary rocks on the Arabian platform are thick and unusually flat. However, several major north-south anticlinal axes above the level of the Arabian platform and some of the larger ones include important oil fields. The origin of the anticlines is uncertain, but there is reason to believe that they are related to some sort of horslike uplift at great depth (Powers et al., 1966).

The crustal structure of the eastern platform seems to have a greater thickness than the western platform by about 5 km. Rodgers et al. (1999) reported that the platform paths are characterized by average sediment and crustal thickness of 4 km and 40 km, respectively. Results of surface wave group velocities and waveform modeling across the Arabian Peninsula (Rodgers et al., 1999) indicate that the Arabian platform can be modeled by two layers, the sedimentary sequence of the upper layer has an average thickness of 4 km and the average P-wave velocity is 4.0 km s^{-1}. The lower layer is 36 km thick with a velocity of 6.3 km s^{-1}. The underlying upper mantle velocity is 8.1 km s^{-i} and the crust-upper mantle boundary is at a depth of about 40 km.

In comparing the derived crustal model of the western Arabian platform with other crustal structures, it is noted that the average crustal velocity (6.2 km s^{-}) is faster than the average crustal velocity obtained by Mokhtar et al. (1992) for the Arabian platform (5.3 kin s^{-1}). The upper crust has velocities in the range of 4.8-6.3 km s^{-1} with a stronger gradient of 0.05 km s^{-1} km^{-1} down to 26 km depth and a weaker gradient of 0.03 km s^{-1} km^{-1} for the lower crust between 26 and 51 km depth. Christensen and Mooney (1995) believe that low crustal velocities in the platform are consistent with a primarily felsic composition.

4. Conclusions

In spite of the non-uniqueness of the spectral analysis method, the present study provides essential information on the manner of specific crustal parameters of the easternmost part of the Arabian Peninsula to fill a gap of regional knowledge. Because of the great disparity of methods used in interpretation of crustal structure data, the comparison and discussion is restricted to that of crustal thicknesses and velocities in relation to the available geological and geophysical data. It should be noted that the identifications of clear-cut P-wave phases may not be possible for ground motions resulting from local or teleseismic earthquakes. Such uncertainty reveals the unwarranted peaks of the observed crustal transfer function ratio.

Generally, the derived model suggests that the crustal thickness and velocity can be resolved within 3 km and 0.3 km s^{-1}, respectively of the observed spectral values. The crust beneath the interior platform beneath Dhahran station consists of five distinct layers. The upper crustal layer has a P-wave velocity of 4.8 km s^{-1} and it is about 8.0 km thick. This velocity represents consolidated and unconsolidated sediments and varies in age from Cambrian to the Quaternary, with some unconformities (ARAMCO, personal communication). The second layer has a velocity of about 5.8 km s^{-I} and 10 km thick, which may represent the upper crystalline basement rocks. The third layer shows a velocity of 6.3 km s^{-1} and 8 km thickness.

The fourth layer shows a P-wave velocity of 6.7 km s^{-1} and thickness of 13 km. The lower layer has a velocity of about 7.4 km s^{-1} and is 12 km thick. The Mohorovicic discontinuity beneath the easternmost Arabian platform indicates a velocity of 8.3 km s^{-1} of the upper mantle at 51 km depth.

Further geophysical work (deep seismic refraction and gravity modeling) between Riyadh and Dhahran is needed to fully understand the lithospheric structure beneath the Arabian platform.

Acknowledgements

We would like to express our thanks and gratitude to the Seismic Studies Center (SSC) of King Saud university for providing earthquake data and original seismograms of Dhahran station.

References

Al-Amri, A.M., Necioglu, A., Mokhtar, T., *1996.* An investigation of crustal and upper mantle structure beneath the Riyadh region from spectral analysis of long period P-wave amplitude ratios. King Abdul Aziz City for Science and Technology Report, vol. *13-46, pp. 175.*

Al-Amri, A.M., *1998.* The crustal structure of the western Arabian platform from the spectral analysis of long-period P-wave amplitude ratios. Tectonophysics *290, 271-283.*

Al-Amri, A.M., *1999.* The crustal and upper mantle structure of the interior Arabian platform. Geophy. J. Int. *136, 421-430.*

Badri, M., *1991.* Crustal structure of central Saudi Arabia, from seismic refraction profiling. Tectonophysics *185, 357-374.*

Bonjer, K.P., Fuchs, K., Wohlenber, J., *1970.* Crustal structure of the east African rise system from spectral response ratios of long-period body waves. Z. Geophys. *36, 287-297.*

Christensen, N., Mooney, W., *1995.* Seismic velocity structure and composition of the continental crust: a global view. J. Geophys. Res. 100, *9761-9788.*

Ellis, R.M., Basham, P.W., *1968.* Crustal characteristics from short-period P-waves. Bull. Seis. Soc. Am. *58, 16811700.*

Hasegewa, H.S., *1971.* Crustal transfer ratios of short and long period body waves recorded at Yellowknife. Bull. Seis. Soc. Am. *61, 1303-1320.*

Haskell, N.A., *1953.* The dispersion of surface waves on multilayered media. Bull. Seis. Soc. Am. *43, 17-34.* IASPEI Software Library, *1990.* Toolbox for plotting and displaying seismic and other data. V. *2.*

IASPEI Software Library, *1992.* Programmable interactive toolbox for seismological analysis (P1TSA), V. *5.* Mellors, R., Vernon, F., Camp, V., Al-Amri, A., Gharib, A., *1999.* Regional waveform propagation in the Saudi Arabian peninsula and evidence for a hot upper mantle under western Arabia. J. Geopys. Res. (in review). Mokhtar, T.A., Maamoun, M., Al-Amri, A.M., *1992.* Seismic structure of the Arabian peninsula from surface waves. King Abdul Aziz City for Science and Technology report, vols. *10-48, pp. 259.*

Mooney, W.D., Gettings, M.E., Blank, H.R., Healy, J., *1985.* Saudi Arabian seismic deep refraction profile, a travel time interpretation for crustal and upper mantle structure. Tectonophysics 111, *173-246.*

Peterson, J.A., Wilson, J.L., *1986.* Petroleum stratigraphy of the northeast Africa-middle east region. In: Hydrocarbon Potential of Intense Thrust Zones, Proc., OAPEC Seminar, December *1986,* Abu Dhabi, vol. II, *pp. 227-330.*

Phinney, R.A., *1964.* Structure of the Earth's crust from spectral behavior of long-period body waves. J. Geophy. Res. *69, 2997-3017.*

Powers, R.W., Ramirez, L.F., Redmond, C.D., Elberg, E.L., 1966. Geology of the Arabian peninsum-sedimentary geology of Saudi Arabia. U.S. Geol. Surv., Profess. Pap. 560-D, 147.

Rodgers, A., Walter, W., Zhang, Y., Mellors, R., Al-Amri, A., 1999. Lithospheric structure within the Arabian peninsula from complete regional waveform modeling and surface wave group velocities. Geophys. J. Int. (in review).

Sandvol, E., Seber, D., Barazangi, M., Vernon, F., Mellors, R., Al-Amri, A., 1998. Lithospheric velocity discontinuities beneath the Arabian shield. Geophys. Res. Lett. 25, 2873-2876.

Seber, D., Vallve, M., Sandvol, E., Steer, D., Barazangi, M., 1997. Middle East tectonics: applications of geographic information systems (GIS). GSA Today 7, 1-6.

Thomson, W.T., 1950. Transmission of elastic waves through a stratified medium. J. Appl. Physics 21, 89.

Turkelli, N., 1984. Seismic investigation of the crustal structure in central Anatolia. Ph.D. thesis, Middle East Tech. Univ., Ankara, Turkey, pp. 78.